SIMULATION ON RED BLOOD CELL'S SEPARATION IN MICROCHANNEL BY USING COMSOL© MULTIPHYSICS

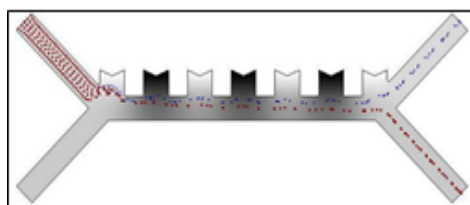Nur Tantiyani Ali Othman*, Halimunnisha Sahul Hameed, Masli Irwan Rosli

Department of Chemical & Process Engineering, Faculty of Engineering and Built Environment, Universiti Kebangsaan Malaysia, 43600, Bangi UKM, Selangor, Malaysia

Graphic Abstract

Abstract

Plasma cell neoplasm disease was caused by the production of large amount of plasma cells which it is unnecessary for the body as it will accumulate in the bone marrow and cause blood thicken and damage the kidneys. Thus, there are several techniques that have been developed for the separation of plasma in blood e.g., viscosity-based sedimentation, size-based filtration, and complete blood count test. Yet, these techniques have some drawbacks such as blood cells easily damaged and do not meet the Point-of-Care (POCT) test features. Hence, in this study, an active separation technique; dielectrophoresis (DEP) force was applied in the X-shaped microchannel which was developed by using AutoCAD© software as it is easily to fabricate at a low cost, while resulting in a high rate of the separation efficiency. The flow profile of a blood distribution and movement along a microchannel was observed by COMSOL© Multiphysics software version 5.5 at various process conditions: blood inlet velocities; V_{IB}=80-200 µm/s, concentration of blood cells; C_{IB}=0.01-0.05 mol/dm³ and electrode voltages; E=-20-20V. It shows that as the inlet velocity is increases, the separation efficiency is increasing. While, as the concentration and electric field intensity is increases, the separation efficiency is decreases due to low DEP force. It shows 100% separation efficiency was obtained for plasma separation at V_{IB}=120 µm/s, C_{IB}= 0.01 mol/dm³, and E=±10V which resulted F_{DEP}=-1.23×10¹⁴ N/m. This DEP separation technique can be applied to improve the efficiency of plasma separation process from blood cells and simultaneously increase the accuracy of the diagnostic.

Keywords: Plasma, microchannel, separation, dielectrophoresis, COMSOL©

Abstrak

Penyakit neoplasma sel plasma adalah disebabkan oleh penghasilan sel plasma yang sangat banyak di mana ia tidak diperlukan oleh badan manusia kerana ia akan menyebabkan penggumpulan protein di sumsum tulang dan merosakkan buah pinggang. Oleh itu, wujudnya beberapa teknik pemisahan sel plasma seperti pemendapan berasaskan kelikatan, penapisan berasaskan saiz, dan ujian kiraan darah penuh. Namun begitu, teknik-teknik ini mempunyai beberapa kelemahan seperti sel darah mudah rosak dan tidak menepati ciri ujian Point-of-Care (POCT). Oleh itu, dalam kajian ini, simulasi teknik pemisahan secara aktif menggunakan daya dielektrophoresis (DEP) dalam saluran mikro berbentuk X dibangunkan menggunakan perisian AutoCAD© kerana ia lebih mudah difabrikasi pada kos yang rendah dan mempunyai kadar keberkesanan pemisahan plasma yang tinggi. Profil aliran bendalir dan pergerakan sel darah di dalam saluran mikro diperhatikan dengan menggunakan perisian COMSOL© Multiphysics versi 5.5 pada pelbagai julat parameter: halaju sel darah di salur

masukan; V_{IB}=80-200 µm/s, kepekatan sel darah di salur masukan; C_{IB}=0.01-0.05 mol/dm³ dan caj voltan elektrod; E=-20-20V. Ia menunjukkan bahawa lebih tinggi halaju sel darah di salur masukan, lebih tinggi kadar keberkesanan pemisahan dicapai. Manakala, semakin tinggi kepekatan sel darah dan caj voltan elektrod yang dikenakan, lebih rendah kadar keberkesanan pemisahan diperolehi disebabkan oleh daya DEP yang rendah. Hasil kajian menunjukkan bahawa kadar keberkesanan 100% proses pemisahan plasma dapat dicapai pada V_{IB}=120 µm/s, C_{IB}=0.01 moldm⁻³ dan E=±10V dengan terhasilnya F_{DEP}=-1.23×10¹⁴ N/m. Teknik pemisahan DEP ini boleh diaplikasi untuk meningkatkan keberkesanan proses pemisahan plasma daripada sel darah dan seterusnya meningkatkan ketepatan analisis penyakit berkaitan sel plasma.

Kata kunci: Plasma, saluran mikro, pemisahan, dielektrophoresis COMSOL©

1.0 INTRODUCTION

Generally, blood cell consists of several components such as plasma, red blood cells, white blood cells and platelets with 50% covered by plasma which is a liquid containing dissolved salts and proteins [1]. The concentrations of major protein groups in a plasma namely albumin, globulin, fibrinogen, salts, glucose, and hormones will change due to the different type of diseases [2]. For instance, as the concentration of potassium in plasma decreases, this condition will lead to the muscle weaknesses and cardiac impulse abnormalities [3]. Thus, it is very important to ensure a level concentration of protein groups in the human blood vessel is in an appropriate composition and in a good condition. Basically, a person can undergo diagnostic tests to detect the disease in their blood vessels if they have any symptoms and preventive measures can be taken accordingly [4].

Mostly, plasma is known as a biomarker to various diseases as it contains a lot of significant information that can be associated with the diagnosis of diseases such as heavy metals namely high blood pressure [5], plasma protein accumulation for chronic kidney diseases [6], DNA concentration in cancer plasma [7] and Alzheimer's disease at different levels [8]. Thus, the process of plasma separation which is also known as plasmapheresis is a very vital before the diagnostic test of the disease is carried out as it can increase the reliability of an analysis [9-10].

Centrifugal method is one of the conventional separation methods which based on the viscosity [11-12]. The plasma separation by centrifugal method is often applied with 5000 rpm speed as it was found to be the optimum speed condition for the separation [13]. Besides, the filtration method also the most used methods to separate plasma from the blood based on particle size [5]. However, it has been found these methods can cause cell lysis as the high centrifugal speeds are used to obtain results rapidly. In addition, the centrifugal method requires a large amount of a sample volume and a high level of skill for operation which makes it inappropriate to be used for on-site analysis [14]. Furthermore, these practical methods use a plasmapheresis machine for plasma separation that is a large and non-portable machine which does not meet the Point-of-Care (POCT) test features [15-18]. Therefore, to overcome these limitations, a microchannel system technology for plasma separation has been introduced as it is portable and less time consuming for performing clinical trials test. This technology has been rapidly developed and applied in medical, biological, physics and chemical industries as it can reduce bulk testing, minimal the costs, easy fabrication and reduce the complexity of the use of tools [19-22].

Chen *et al*. designed a microchannel that made from polydimethylsiloxane (PDMS) and glass substrate with stacked microbeads to study the trajectory of red blood cells where the plasma will be flowing to the separation channel [23]. They found the distance between microbeads should be smaller which is 10µm to trap the red blood cells efficiently. As well, Zhong *et al*. studies the hydrodynamic effect on the flow rate of blood and obstacles to separate the plasma from blood by using sedimentation-based separation [24]. The obstacles was designed as the narrow bifurcation region will create the centrifugal force that formed a cell free layer known as plasma where it can be separated at the inlet flow rate of 3µL/min. Guan *et al*. analyzed platelet separation in zigzag shaped microchannel using dielectrophoresis (DEP) force at numerous parameters range such as the channel angle (θ=60-150°), inlet channels velocity ratio (v_r=1:1-1:4), electrical voltage (E=11-23V) and frequency (f=10⁻³-10⁶ Hz) for platelet cells separation process [25]. Their finding shows that 99.4% of platelet separation efficiency was achieved due to the usage of DEP force at the electrode voltage of 20V that creates a non-uniform electric field. Besides, Oshii K. *et al*. and Othman *et al*. were applied DEP force to observe the particle flow profile distribution, and separation in the X-shaped microchannel [26-27].

Yet, DEP force has been developed and utilized in the microchannel system for a very long time ago, nonetheless only a few studies have been reported for the separation of plasma from blood cell due to the complexity on the device's design that need to be integrated and time constraint for performing the

experimental analysis [24, 28-31]. Additionally, the experimental study requires high cost for fabrication process and the optimization of separation process is hard to be achieved as it is difficult to control the surroundings accurately. Therefore, in this study, X-shaped microchannel was developed via AutoCAD© 2018 and COMSOL© Multiphysics version 5.5 software to observe and determine the efficiency of plasma separation from blood cell by using DEP force. By carrying out the simulation, the flow profile along the microchannel was observed at different condition of inlet velocities of blood cells (v_{IB}=80-200 μm/s), inlet concentration of blood cells (C_{IB}=0.01-0.05 mol/dm^3) and electrical voltage of electrodes (E=±20V). From these range of parameters, the efficiency of the plasma separation process was determined at the outlets of the microchannel.

The flow inside a microchannel is subjected to Navier-stokes equation where a blood's condition is incompressible and non-Newtonian fluid. Generally, DEP force is applied to separate neutral particles in a liquid medium based on particles and medium polarization inside a non-homogenous electric field [21]. When the particles with different dielectric properties are suspended in an electric field, it will result in a polarization where the magnitude and the direction of the induced dipole depends on the frequency and magnitude of the supplied electric field [32]. If the value of DEP force is positive, particles will be pushed towards the electric field, while if it is negative, the particles will be pushed away from the electric field [34].

Equation 1 shows the DEP force acted on the particles where ε_m is a relative permittivity of medium, r is a particle radius, E_{rms} is a root mean square of electric field, $Re(f_{CM})$ is a Clausius-Mossotti (CM) factor which will determine the value of the positive or negative DEP of the particle. Equation 2 is used to calculate the CM factor where ε_{p*} and ε_{m*} are a complex permittivity of particle and medium, respectively which depends on electric conductivity and frequency of AC electric field, ω is the angular frequency, ε and σ are permittivity and conductivity of the respective particle and medium.

$$F_{DEP} = 2\pi\varepsilon_m r^3 Re\,(f_{CM})\nabla|E_{rms}|^2 \quad (1)$$

$$Re(f_{CM}) = \frac{\varepsilon_p^* - \varepsilon_m^*}{\varepsilon_p^* - 2\varepsilon_m^*}, \qquad \varepsilon^* = \varepsilon - j\frac{\sigma}{\omega} \quad (2)$$

2.0 METHODOLOGY

In the simulation, firstly the X-shaped microchannel was designed based on studies carried out by Zhang Y. & Chen X. where the length of the main channel is 625 μm to provide broad surface interface for the formation of cell free layer, while the height and the width of the inlet and outlet channels is 40 μm to ensure the laminar flow (Re<1) of the fluid flowed inside the microchannel [34]. Figure 1 shows the 2D X-

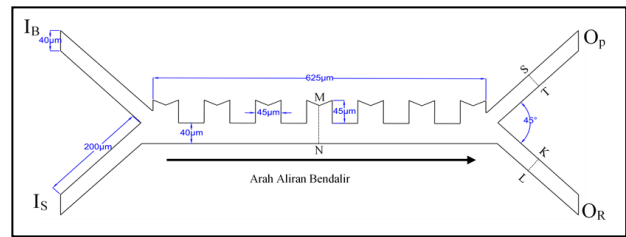shaped microchannel that was developed and modelled using AutoCAD© 2018 software.

Figure 1 The 2D X-shaped microchannel model

This design was selected as its ability to separate plasma from blood cell in a more accurate result. This microchannel has two inlets, I_B and I_S for feed of the blood cell and PBS buffer solution, respectively and two outlets, O_P and O_R for flow out of the plasma and red blood cells, respectively. This channel has been modelled and built up with seven electrodes where its height and length are 45 μm. To analyze the effect of DEP force on the blood cell particles movement and separation efficiency, the cross-sections of the middle channel flow (M-N), outlet area; O_P (S-T) and O_R (K-L) inside the microchannel were chosen where the M-N point is located at center of the straight channel, while point S-T and K-L is located at center channel near to the outlets area.

In this study, blood is used as fluid flowing through the inlet I_B, while PBS solution used as buffer flowing through I_S. Then, the plasma will be separated from the blood flow at the outlet area due to the charged of the DEP force on the electrodes. The plasma will flow out through the upper outlet channel, while the remain blood compositions will flow out at the lower outlet channel. The properties of the materials are shown as in Table 1 [35].

Table 1 The properties of red blood cells, plasma, and PBS buffer solution [35]

Properties	RBC	Plasma	PBS
Density (kg/m^3)	1095	1000	1010
Viscosity (cp)	3.0	1.35	1.05
Particle diameter (μm)	6.0	1.0	0.2
Conductivity (S/m)	0.31	0.055	1.0
Relative permittivity (F/m)	55	80	80

Before proceeding to simulate and analysis the data, a mesh independency test was carried out on the designed 2D X-shaped microchannel to obtain the optimum mesh size where three types of mesh; fine, normal, and coarse mesh were selected. The result of the mesh independency test in a Figure 2 shown that a normal mesh is the optimum mesh size as the peak velocity at y=20 μm is almost similar with the fine mesh; v=0.00144 m/s and v=0.00142 m/s for normal mesh and fine mesh, respectively. It shows with this normal mesh, it is just adequate to obtain a high accuracy result with 2% different as compared

to the course mesh. Besides, this microchannel model also had been validated and verified with the others channel designed by Zhang Y. & Chen X. [34]. And, it shown a similar pattern on the result of the electric field distribution where the voltage is higher under the positively charged electrode, while the voltage is lower under the negatively charged electrode.
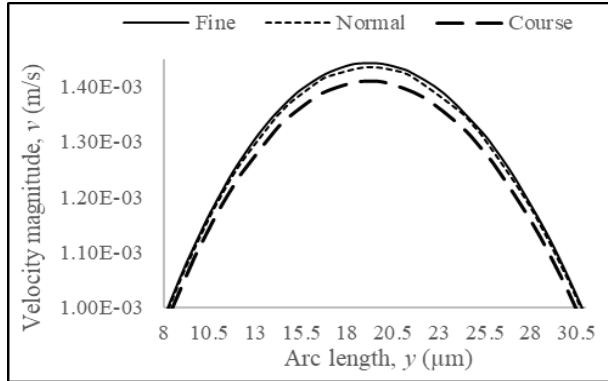

Figure 2 The mesh independency test on velocity magnitude

In the COMSOL© Multiphysics, four physics modules were chosen to simulate and analysis the plasma separation process in the microchannel which is a creeping flow module to specify the fluid flow, a transport of diluted species module to specify the fluid concentration, AC/DC electric current module to visualize electric field charged in the microchannel and particle trajectories module to observe particle movement and analyze the efficiency of separation process. The pressure inside the microchannel is set up at 1 atm, the channel wall is set to bounce the particles, while the fluid velocity is assumed to be in a laminar flow and a drag force is based on the Stokes' principle. The inlet velocity and concentration of the blood feed was fixed at v_{IB}=800 µm/s and C_{IB}=0.01 mol/dm³ to observe velocity flow and concentration distribution profile, respectively. The simulation was carried out by injecting 610 number of blood cells (1:1 ratio of red blood cells to plasma) through upper inlet, I_B and PBS buffer solution at the lower inlet, I_S. To determine the efficiency of the plasma separation, the inlet blood velocity, v_{IB} was manipulated at 80, 120,160 and 200 µm/s with the PBS inlet velocity was remain constant at v_{IS}=800 µm/s. Then, the velocity distribution in the microchannel was observed in a wide range of a blood cell concentration at the inlet, C_{IB}=0.01, 0.02, 0.03, 0.04 and 0.05 mol/dm³ with the concentration of PBS solution was remain constant at C_{IS}=0.01 mol/dm³. Finally, the effect of DEP force on the efficiency of plasma separation was observed at several voltage charged on the electrodes, E=-20V to 20V.

3.0 RESULTS AND DISCUSSION

Figure 3 shows the flow profile of the mixture velocity distribution in the microchannel where the inlet blood velocity was manipulated at four velocity ranges; v_{IB}=80, 120, 160 and 200 µm/s, while the inlet velocity of PBS solution was remained constant at v_{IS}=800 µm/s. The color bar indicated the average of mixture velocity flow distribution of fluid in the microchannel which can be visualized by the red and blue color, respectively.
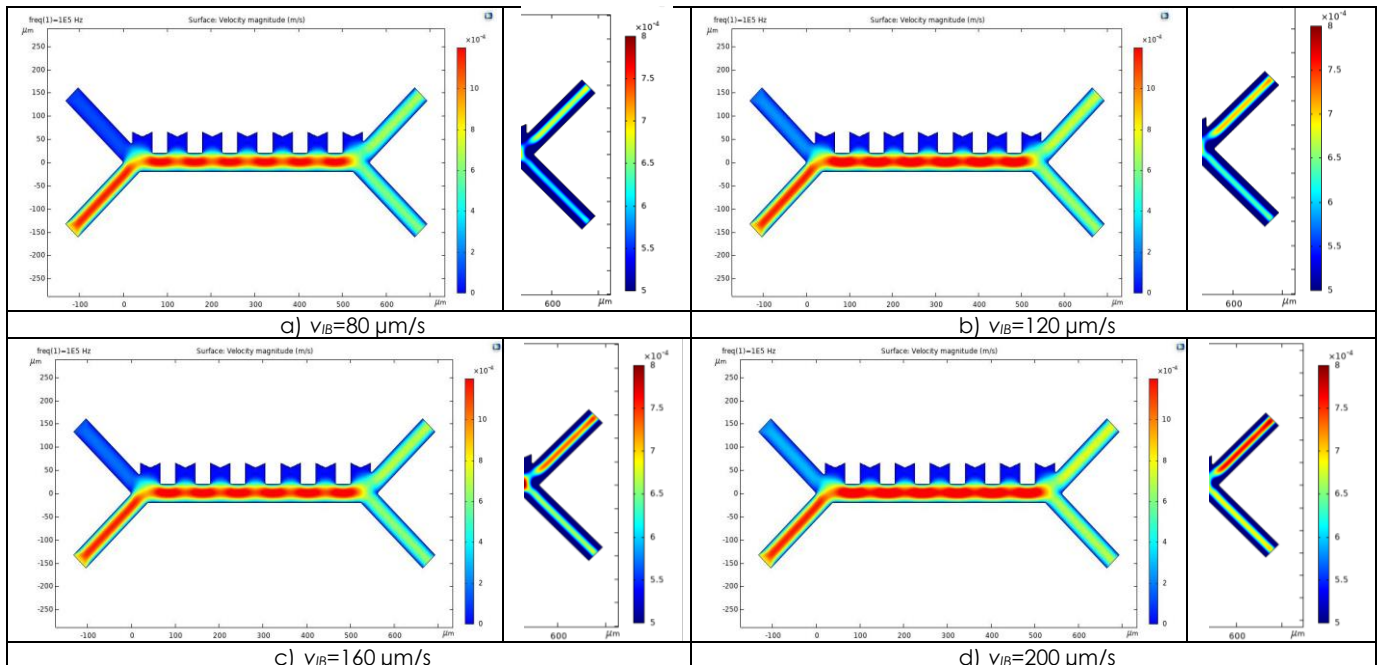

Figure 3 The mixture of velocity profile in the microchannel at different inlet velocities; v_{IB}=80-200 µm/s

The left-side figure shows the overall view of the average mixture velocity flow profile along the microchannel, with the highest velocity is at v=1200 µm/s, while the lowest velocity is v=0 m/s. Meanwhile, the right-side figure shows the cross-section view at the outlets channel for better observation on the velocity flow profile near to the outlets area with the highest velocity is at v=800 µm/s, while the lowest velocity is at v=500 µm/s which can be visualized by the red and blue color, respectively.

It shows as the higher of the inlet blood velocity, the mixture velocity profile at the outlet O_R is also increases and has been distributed equally from the center to the channel wall area. For instance, at the lowest velocity; v_{IB}=80 µm/s, the average mixture of velocity distribution flow profile at the upper outlet velocity is v_{OR}=609 µm/s, while at highest velocity; v_{IB}=200 µm/s, the average mixture velocity is v_{OR}=692 µm/s. The variance results on the mixture velocity observation are occurred due to the changes in a pressure and inertia in the channel and as stated in Bernoulli principle, pressure is inversely proportional to the velocity of fluid [27, 36].

Meanwhile, Figure 4 shows the velocity magnitude for all four velocities range where the peak velocity is shown at x=20 µm which is at the center of straight channel at the M-N cross-section. It was observed that the highest velocity inlet will be resulted with the highest mixture of velocity distribution flow profile in the microchannel due to movement and interaction of particles in the channel flow.
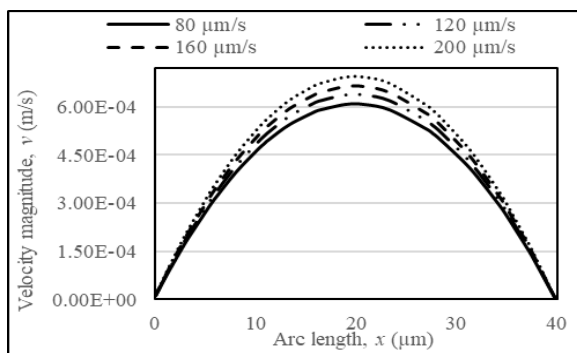
Figure 4 The velocity magnitude against arc length different inlet velocities; v_{IB}=80-200 µm/s

From the mixture velocity distribution and particle trajectories observation, the efficiency of the plasma separation process was then determined based on the number of cells as shown in a Figure 5 where the constant curve shows that the separation process has been fully achieved and completed. The results show almost all the plasma cells at t=10s have been successfully separated since the curve is remain constant for all inlet blood velocities. Besides, as the simulation was carried out by injecting 610 number of blood cells (1:1 ratio of red blood cells to plasma) through inlets, it shows 100% separation efficiency has been achieved as the total number of cells at lower

part of channel outlet, N_{OR}=305 cells when the inlet blood velocity is at above 120 µm/s. From this result, it shows v_{IB}=120 µm/s is the optimum velocity as it shows the shortest time to separate the plasma which it will lead to the deformation of the blood cells [37].
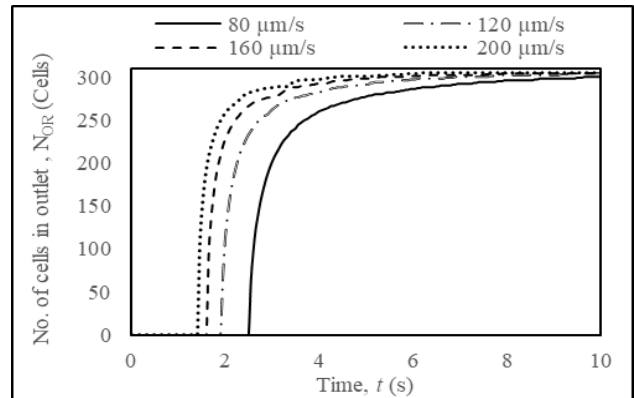
Figure 5 The number of cells in the outlet OR at different inlet velocities; v_{IB}=80-200 µm/s

Figure 6 shows the concentration distribution flow profile in the microchannel as the inlet concentration of blood cell was manipulated at five concentrations range of C_{IB}=0.01, 0.02, 0.03, 0.04 and 0.05 moldm^{-3}, while the inlet concentration of PBS solution was remained constant at the concentration of C_{IS}=0.01 moldm^{-3}. The color bar shows the distribution of the fluid mixture concentration inside the microchannel, where the highest concentration is C=0.05 moldm^{-3}, while the lowest concentration is C=0.01 moldm^{-3}, which can be visualized with a red and blue color, respectively. It shows as the inlet blood concentration is increases, the concentration flow profile at cross-sections M-N and S-T also increases as the mixture concentration of blood cell and PBS have been distributed in the channel as the mixture solution flow through the microchannel.

Figure 7 shows the concentration flow distribution magnitude at the outlet area at the cross-section M-N, C_{M-N} and S-T, C_{S-T} along the arc length, y of microchannel at various range of inlet concentration of blood cell; C_{IB}=0.01-0.05 moldm^{-3}. For instance, in the Figure 7a) at C_{IB}=0.02 moldm^{-3}, the concentration at the cross-section M-N at y=0 µm is C_{M-N}=0.0125 moldm^{-3}. While, at C_{IB}=0.05 moldm^{-3}, it is increases, however there are slightly small differences at the position of y=20 µm, where the concentration value are 0.013 moldm^{-3} and 0.011 moldm^{-3}, respectively. Whereas, in the Figure 7b) at C_{S-T}, the concentration at y=0 µm is C_{S-T}=0.0135 moldm^{-3} at C_{IB}=0.02 moldm^{-3}, whereas at C_{IB}=0.05 moldm^{-3}, the concentration at the center of microchannel is increases but like C_{M-N} where there are slightly some differences at y=40 µm where the concentration value are 0.015 moldm^{-3} and 0.011 moldm^{-3}, respectively.
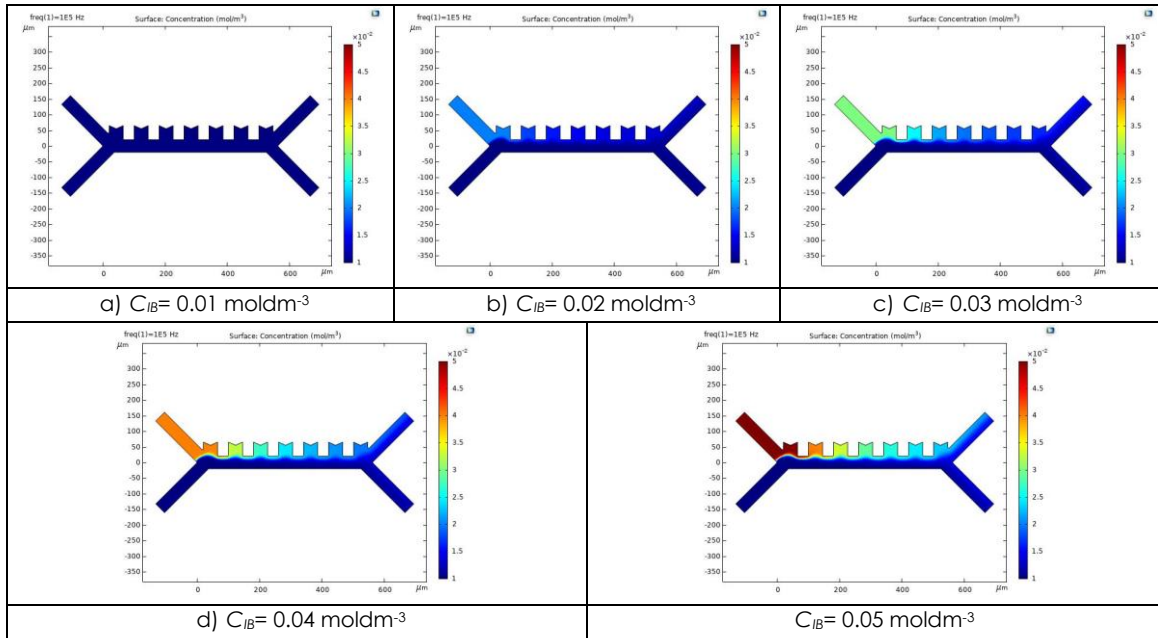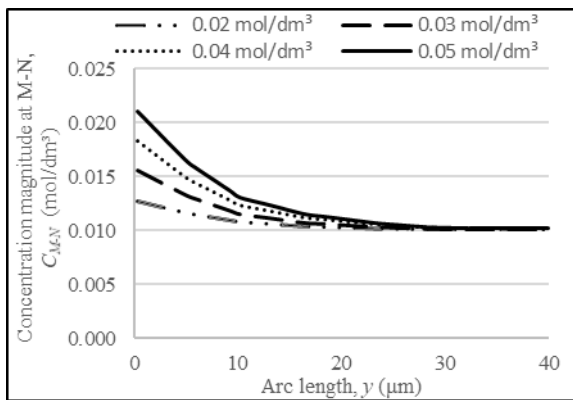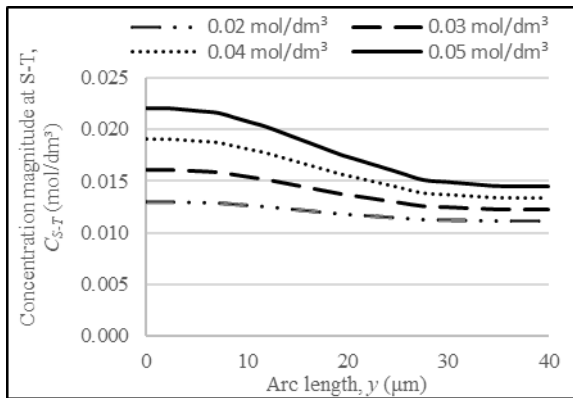
Figure 6 The concentration distribution profile in the microchannel at five range of the inlet concentrations; 0.01-0.05 moldm^{-3}

Figure 7 The concentration magnitude at a) M-N, C_{M-N} and b) S-T, C_{S-T} along the arc length, y of microchannel

This is happened due to the dense concentration is related to a blood viscosity and density as stated in the Navier-Stokes's equation, whereas as the higher concentration, the fluid's viscosity and density is also higher [38]. This hypothesis is also supported by Murali C. & Nithiarasu P., where there is accumulation of red blood cells due to lower shear rate at the center of microchannel as compared to the wall [39]. Thus, the optimum inlet blood concentration is at C_{IB}=0.01 moldm^{-3} as the higher concentration will lead to the blood's clogging inside the microchannel due to the accumulation of red blood cells at the bottom of the channel.

To observe the effect of DEP force on the particle movement and distribution that flowed inside the microchannel, the electrodes were charged with positive and negative charge aside between E=-20V to E=20V. This value range of the electrical charged on the electrodes are selected as the higher voltage and centrifugal speed can cause blood cell lysis and will damage the blood cell.

Figure 8 shows result observation on the effect of the electric field distribution in the microchannel flow at various range of voltage charged at the seven electrodes (electrode A-G) where positive voltages of E=5, 10, 15 and 20V were charged at electrodes A, C, E and G, while the negative voltages of E=-20, -15, -10 and -5V were charged at electrodes B, D and F. The color bar shows the electric field intensity in the microchannel where the highest voltage is 20V (red color), while the lowest voltage is -20V (blue color).
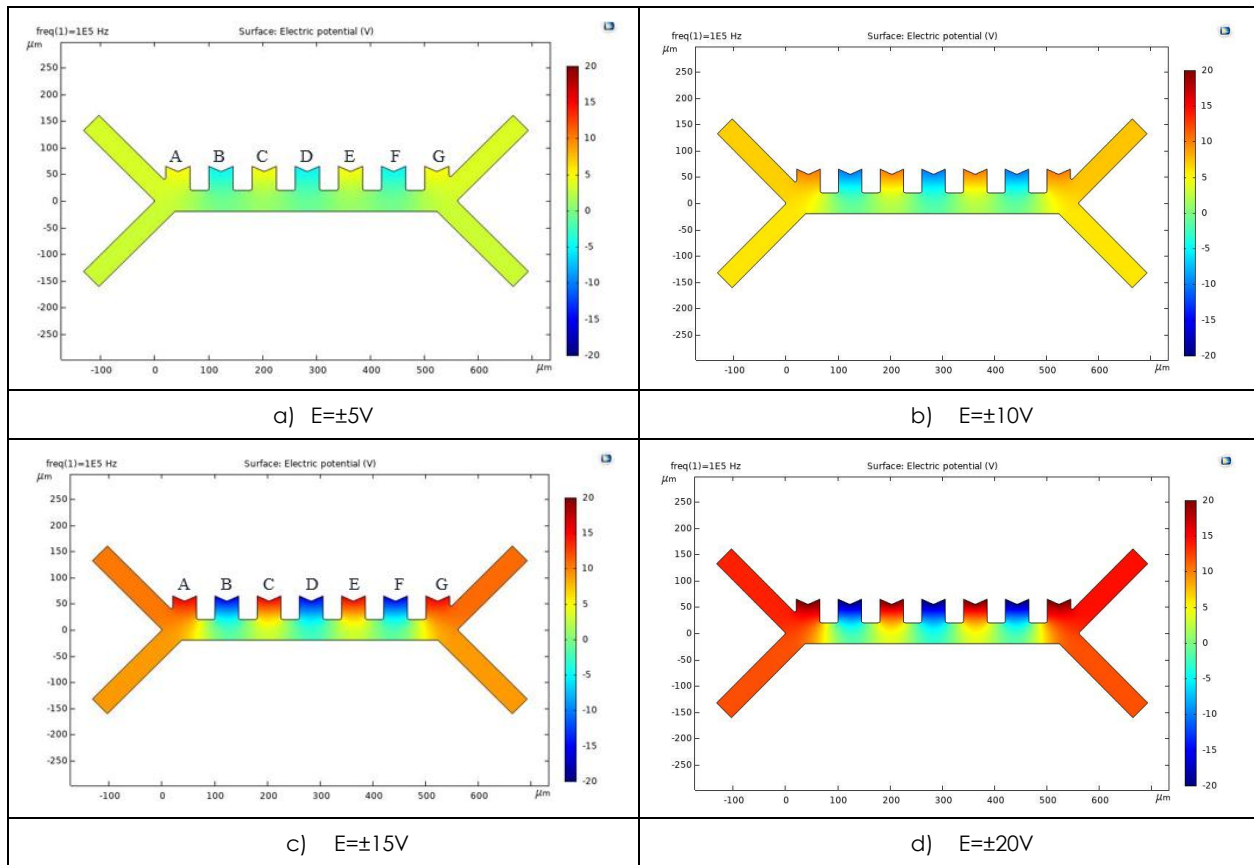
Figure 8 The electric field distribution in the microchannel at different electrode voltage
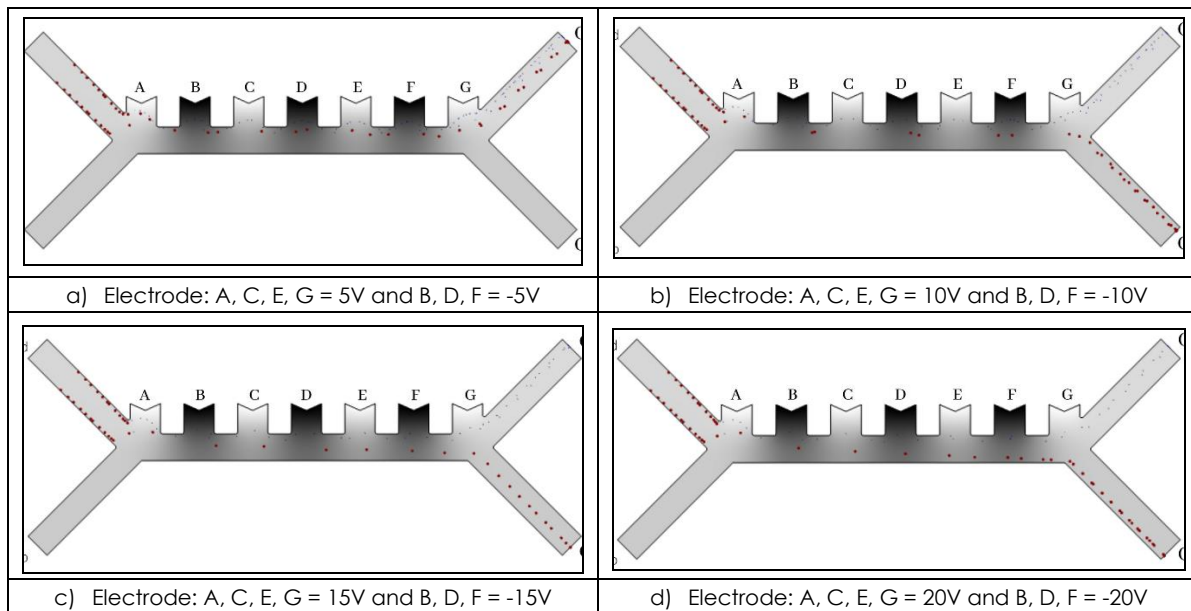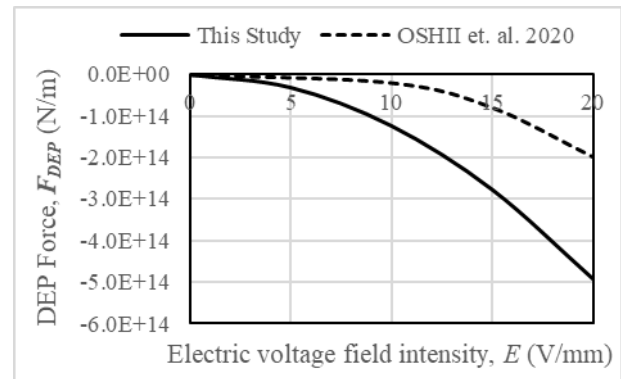

Figure 9 The particle trajectories in the microchannel at different electrode voltage

It shows as the higher voltage charged at the electrodes; the voltage distribution is decreases as its distance away from the electrodes. This reduction on the voltage distribution is occurred due to the voltage on the electrode being higher than the voltage inside the microchannel flow. From these simulation results, the effect of the electrode voltage charged on the blood separation was determined by observation on the particle trajectories distribution as shown in a Figure 9 at various range of the electrode voltage; E=±5 to ±20V at the seven electrodes where the positive voltages of E=5-20V were charged at the electrodes A, C, E and G, while negative voltages of E=-20V-5V were charged positive at the electrodes B, D and F. The red dotted in the figure is refer to the red blood cells, while the blue dotted is the plasma cells. The results show that the particles have been moved further away at the outlets area as the higher the voltage was charged on the electrode. For an example, when the electrodes were charged at E=±5V as shown in the Figure 9a), the particles are unable to be separated due to insufficient required voltage inside the microchannel which is quite lower than the voltage specified on the electrode.

However, as the electrode is charged more than E>±5V, it shows the particles slightly move further away from the center channel and as the voltage is keep increased at E=±20V as shown in Figure 9d), the alignment of particle is nearer to the channel wall of the lower outlet, O_R was observed. Based on this simulation results, it can be observed that the red blood cells had been moved further away from the electrode charged due to the nDEP force. The red blood cells moved away from the separation region and flow together into the PBS solution which then flowed out to the exit through the outlet O_R. The plasma will remain in the separation region as the cells are attracted to the electrode due to the DEP force. Then, the plasma will continuously be flowing in the separation region and proceed to exit through the upper outlet at O_P.

As well, to verify and validate all these simulation results of the DEP force, the DEP force is calculated based on Equations (1) and (2) and then, it was compared with the experimental results by Oshii K. et. al [26] as shown in a Figure 10. It shows a similar trend of pattern where the DEP force is decreases as the electric field intensity in a microchannel increase as from the Equation (1), it stated that the electric field intensity is exponentially proportional to the DEP force.

Besides, the smaller particle size also results in the lower DEP force since the DEP force of the smaller particle is relatively weaker [40]. This simulation result shows at E=5 V/mm, the maximum DEP force was determined which is F_{DEP}=-3.08×10^{13} N/m. However, it shows that the particles are not separated at E=5 V/mm due to insufficient of the DEP force. Thus, it can be concluded the optimum electric field intensity will be at E=10 V/mm where F_{DEP}=-1.23×10^{14} N/m since it resulted with the highest DEP force that also shown 100% separation efficiency was achieved.

Figure 10 Validation of the DEP force, FDEP (N/m) against electric field intensity, E (V/mm) with Oshii *et al.*

From the particle trajectory and results observation, the separation efficiency was determined based on the ratio of number of cells in the outlet to the inlet feed as shown in a Figure 11. It shows the optimum inlet blood velocity is obtained at v_{IB}=120 μm/s, while the optimum inlet PBS velocity is at v_{IS}=800 μm/s since 100% of separation efficiency was achieved where all 305 number of the red blood cells are successfully separated from the plasma. The optimum inlet blood concentration is observed at C_{IB}=0.01 mol/dm^3 since the difference in the inlet concentration between the blood cells and PBS will increase the resistance for the buffer solution to mix up with the red blood cells inside the microchannel [38].
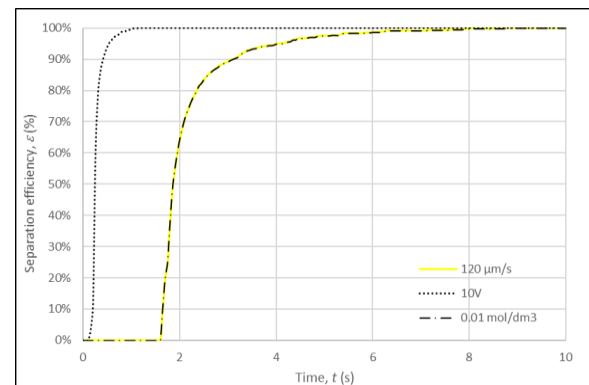
Figure 11 The separation efficiency with respect of time

This result shows the DEP force plays an important role in the plasma separation process since the time taken to achieve 100% separation to occur is within *t*=1s which is the shortest time as compared to the others inlet concentration and velocity at *t*=7.5s. This is occurred due to the arrangement of the positive and negative electrode is side by side electrodes to create a non-homogenous electric field that can separate particles with different dielectric properties such as plasma and red blood cells. The value of the DEP force is indicated the highest since the particle

with smaller size has weaker DEP force, thus more required DEP force to move the particles away to the other end of the microchannel [39].

4.0 CONCLUSION

The 2D X-shaped microchannel has been successfully designed and developed to observe the effects of inlet blood velocity, inlet blood concentration and the electrodes voltage charged on the plasma separation process. The simulation results show that the optimum blood inlet velocity is obtained at inlet velocity of v_{IB}=120 µm/s in order to reduce the inertia and pressure inside the microchannel that can result in deformation of blood cells. The optimum inlet blood concentration is at C_{IB}=0.01 mol/dm^3 to obtain better mixing and avoid accumulation of blood cells from clogging in the microchannel. The optimum electrode voltage for plasma separation process is at E=10 V/mm as it shows the highest DEP force, F_{DEP}=-1.23×10^{14} N/m with 100% of separation efficiency rate. These simulation results on the DEP force shows the similar pattern as compared with Oshii K. *et al.* proving that the results is validated and can be applied further to determine the plasma separation in the medical field industry.

Acknowledgement

References

[1]   Avsievich, T., Zhu, R., Popov, A., Bykov, A. and Meglinski, I. 2020. The Advancement of Blood Cell Research by Optical Tweezers. *Reviews in Physics*. 100043.
DOI: http://dx.doi.org/10.1016/j.revip.2020.100043.

[2]   Huang, C. Te, Li, P. N., Pai, C. Y., Leu, T. S. and Jen, C. P. 2010. Design and Simulation of a Microfluidic Blood-Plasma Separation Chip Using Microchannel Structures. *Separation Science and Technology*. 45(1): 42-49.
DOI: http://dx.doi.org/10.1080/01496390903402125.

[3]   Stein, E. A. and Pum, J. 2004. Blood and Plasma. *Encyclopedia of Analytical Science*. Second Edition. 2: 294-300.
DOI: http://dx.doi.org/10.1016/B0-12-369397-7/00047-9.

[4]   Feher, J. 2012. Plasma and Red Blood Cells. *Quantitative Human Physiology*. 428-436.
DOI : http://dx.doi.org/10.1016/b978-0-12-382163-8.00045-1.

[5]   Marieb, E. N. and Hoehn, K. 2012. Overview: Blood Composition and Functions. *Human Anatomy & Physiology*. 634-657. Retrieved from http://www.phschool.com/atschool/florida/pdfbooks/sci_Marieb/pdf/Marieb_ch17.pdf.

[6]   Luczak, M., Formanowicz, D., Pawliczak, E., Wanic-Kossowska, M., Wykretowicz, A. and Figlerowicz, M. 2011. Chronic Kidney Disease-Related Atherosclerosis - Proteomic Studies of Blood Plasma. *Proteome Science*. 9: 1-12.
DOI: http://dx.doi.org/10.1186/1477-5956-9-25.

[7]   Hainaut, P. 2000. Detection of Circulating Tumour DNA in the Blood of Cancer Patients. *Medecine/Sciences*. 16(3): 446.
DOI: http://dx.doi.org/10.4267/10608/1670.

[8]   Carmona, P., Molina, M., Calero, M., Bermejo-Pareja, F., Martínez-Martín, P. and Toledano, A. 2013. Discrimination Analysis of Blood Plasma Associated with Alzheimer's Disease Using Vibrational Spectroscopy. *Journal of Alzheimer's Disease*. 34(4): 911-920.
DOI: http://dx.doi.org/10.3233/JAD-122041.

[9]   Bhuvanendran Nair Gourikutty, S., Chang, C. P. and Puiu, P. D. 2016. Microfluidic Immunomagnetic Cell Separation from Whole Blood. *Journal of Chromatography B: Analytical Technologies in the Biomedical and Life Sciences*. 1011: 77-88.
DOI: http://dx.doi.org/10.1016/j.jchromb.2015.12.016.

[10] Nakashima, Y., Hata, S., Yasuda, T., Mohamed Zackria, M. Z. A., Tirth, V., Yousuff, C. M., Shukla, N. K., *et al.* 2020. Blood Plasma Separation and Extraction from a Minute Amount of Blood Using Dielectrophoretic and Capillary Forces. *Journal of the Brazilian Society of Mechanical Sciences and Engineering*. 42(4): 561-569.
DOI: 10.1109/SENSORSNANO44414.2019.8940041.

[11] Basu, D. and Kulkarni, R. 2014. Overview of Blood Components and Their Preparation. *Indian Journal of Anaesthesia*. 58(5): 529-537.
DOI: http://dx.doi.org/10.4103/0019-5049.144647.

[12] Maria, M. S., Chandra, T. S. and Sen, A. K. 2017. Capillary Flow-Driven Blood Plasma Separation and On-Chip Analyte Detection in Microfluidic Devices. *Microfluidics and Nanofluidics*. 21(4): 1-21.
DOI: http://dx.doi.org/10.1007/s10404-017-1907-6.

[13] Rhoades, T., Kothapalli, C. R. and Fodor, P. S. 2020. Mixing Optimization in Grooved Serpentine Microchannels. *Micromachines*. 11(1): 1-12.
DOI: http://dx.doi.org/10.3390/mi11010061.

[14] Zhang, J., Wei, X., Xue, X. and Jiang, Z. 2014. Structural Design of Microfluidic Channels for Blood Plasma Separation. *Journal of Nanoscience and Nanotechnology*. 14(10): 7419-7426.
DOI: http://dx.doi.org/10.1166/jnn.2014.9559.

[15] Dauson, E., Gregory, K., Oppenheim, I. and Dahl, K. 2017. Human Blood Cell Separation Using Bulk Acoustic Waves in a Machined PMMA Microchannel. *IEEE International Ultrasonics Symposium*. IUS 0-3.
DOI: http://dx.doi.org/10.1109/ULTSYM.2017.8092782

[16] Kuan, D. H., Wu, C. C., Su, W. Y. and Huang, N. T. 2018. A Microfluidic Device for Simultaneous Extraction of Plasma, Red Blood Cells, and On-Chip White Blood Cell Trapping. *Scientific Reports*. 8(1): 1-9.
DOI: http://dx.doi.org/10.1038/s41598-018-33738-8.

[17] Li, D., Chen, H., Ren, S., Zhang, Y., Yang, Y. and Chang, H. 2020. Portable Liquid Chromatography for Point-Of-Care Testing of Glycated Hemoglobin. *Sensors and Actuators, B: Chemical*. 305(September 2019): 127484.
DOI: http://dx.doi.org/ 10.1016/j.snb.2019.127484.

[18] Mohamed Zackria, M. Z. A., Tirth, V., Yousuff, C. M., Shukla, N. K., Islam, S., Irshad, K. and Aarif, K. O. M. 2020. Simulation Guided Microfluidic Design for Multitarget Separation Using Dielectrophoretic Principle. *Biochip Journal*. 14(4): 390-404.
DOI: http://dx.doi.org/10.1007/s13206-020-4406-x.

[19] Pandey, C. M., Augustine, S., Kumar, S., Kumar, S., Nara, S., Srivastava, S. and Malhotra, B. D. 2018. Microfluidics Based Point-of-Care Diagnostics. *Biotechnology Journal*. 13(1): 1-11.
DOI: http://dx.doi.org/10.1002/biot.201700047.

[20] Baek, S., Radebaugh, R. and Bradley, P. E. 2020. A New Method for Heat Transfer Coefficient Measurements of

Single-Phase Fluids During Laminar Flow in Microchannels. *International Journal of Heat and Mass Transfer*. 157. DOI: 10.1016/j.ijheatmasstransfer.2020.119891.

[21] Mitra, P., Dutta, S., Nagahanumaiah and Hens, A. 2020. Separation of Particles in Spiral Micro-Channel Using Dean's Flow Fractionation. *Journal of the Brazilian Society of Mechanical Sciences and Engineering*. 42(8): 1-12. DOI : http://dx.doi.org/10.1007/s40430-020-02482-4.

[22] Shah, I., Kim, S. W., Kim, K., Doh, Y. H. and Choi, K. H. 2019. Experimental and Numerical Analysis of Y-Shaped Split and Recombination Micro-Mixer with Different Mixing Units. *Chemical Engineering Journal*. 358: 691-706. DOI: http://dx.doi.org/10.1016/j.cej.2018.09.045.

[23] Chen, M. Di, Yang, Y. T., Deng, Z. Y., Xu, H. Y., Deng, J. N., YANG, Z., HU, N., *et al.* 2019. Microchannel with Stacked Microbeads for Separation of Plasma from Whole Blood. *Chinese Journal of Analytical Chemistry*. 47(5): 661-668. DOI: http://dx.doi.org/10.1016/S1872-2040(19)61157-6.

[24] Zhong, R., Wu, N. and Liu, Y. 2019. Microfluidic Human Blood Plasma Separation for Lab on Chip Based Heavy Metal Detections. *ECS Transactions*. 41(38): 11-16. DOI: http://dx.doi.org/10.1149/1.3697855.

[25] Guan, Y., Liu, Y., Lei, H., Liu, S., Xu, F., Meng, X., Bai, M., *et al.* 2020. Dielectrophoresis Separation of Platelets Using a Novel Zigzag Microchannel. *Micromachines*. 11(10). DOI: http://dx.doi.org/10.3390/mi11100890.

[26] Oshii, K., Je-Eun CHOI, Obara, H. and Takei, M. 2010. Measurement of Dielectrophoretic Velocities of Microparticles in a Minichannel. *Journal of the Japanese Society for Experimental Mechanics*. 10: s79-s84. DOI: http://dx.doi.org/10.11395/jjsem.10.s79.

[27] Othman, N., T., A. and Lee, C. S. 2021. Simulation Study on the Effect of Dielectrophoresis Force on a Separation of Platelet from Blood Cell in a 3D Mini Channel. *Journal Engineering*. 33(2): 249-255. DOI: http://dx.doi.org/10.17576/jkukm-2021-33(2)-08.

[28] Gifford, S. C., Strachan, B. C., Xia, H., Vörös, E., Torabian, K., Tomasino, T. A., Griffin, G. D., *et al.* 2018. A Portable System for Processing Donated Whole Blood into High Quality Components Without Centrifugation. *PLoS ONE*. 13(1): 1-20. DOI: http://dx.doi.org/10.1371/journal.pone.0190827.

[29] Kim, J., Antaki, J. F. and Massoudi, M. 2016. Computational Study of Blood Flow in Microchannels. *Journal of Computational and Applied Mathematics*. 292(July): 174-187. DOI: http://dx.doi.org/10.1016/j.cam.2015.06.017

[30] Tripathi, S. & Agrawal, A. 2020. Blood Plasma Microfluidic Device: Aiming for the Detection of COVID-19 Antibodies Using an On-Chip ELISA Platform. *Transactions of the Indian National Academy of Engineering*. 5(2): 217-220.

DOI: http://dx.doi.org/10.1007/s41403-020-00123-9.

[31] Yang, F., Zhang, Y., Cui, X., Fan, Y., Xue, Y., Miao, H. and Li, G. 2019. Extraction of Cell-Free Whole Blood Plasma Using a Dielectrophoresis-Based Microfluidic Device. *Biotechnology Journal*. 14(3). DOI: http://dx.doi.org/10.1002/biot.201800181.

[32] Pohl, H. A., Pollock, K. and Crane, J. S. 1978. Dielectrophoretic Force: A Comparison of Theory and Experiment. *Journal of Biological Physics*. 6(3-4): 133-160. DOI: http://dx.doi.org/10.1007/BF02328936.

[33] Yang, J. 1999. Cell Separation on Microfabricated Electrodes Using Dielectrophoretic/Gravitational Field-Flow Fractionation. *Analytical Chemistry*. 71(5): 911-918. DOI: http://dx.doi.org/10.1021/ac981250p.

[34] Zhang, Y. and Chen, X. 2020. Dielectrophoretic Microfluidic Device for Separation of Red Blood Cells and Platelets: A Model-Based Study. *Journal of the Brazilian Society of Mechanical Sciences and Engineering*. 42(2). DOI: http://dx.doi.org/10.1007/s40430-020-2169-x.

[35] Meijer, H. E. H., Singh, M. K., Kang, T. G., Den Toonder, J. M. J. and Anderson, P. D. 2009. Passive and Active Mixing in Microfluidic Devices. *Macromolecular Symposia*. 279(1): 201-209. DOI: http://dx.doi.org/10.1002/masy.200950530.

[36] Tripathi, S., Varun Kumar, Y. V. B., Prabhakar, A., Joshi, S. S. and Agrawal, A. 2015. Passive Blood Plasma Separation at The Microscale: A Review of Design Principles and Microdevices. *Journal of Micromechanics and Microengineering*. 25(8): 83001. DOI: http://dx.doi.org/10.1088/0960-1317/25/8/083001.

[37] Luo, T., Fan, L., Zeng, Y., Liu, Y., Chen, S., Tan, Q., Lam, and R. H. W., 2018. A Simplified Sheathless Cell Separation Approach Using Combined Gravitational-Sedimentation-Based Prefocusing and Dielectrophoretic Separation. *Lab on a Chip*. 18(11): 1521-1532. DOI: http://dx.doi.org/10.1039/c8lc00173a.

[38] Chandran, K., Dalal, I. S., Tatsumi, K. and Muralidhar, K. 2020. Numerical Simulation of Blood Flow Modeled as A Fluid- Particulate Mixture. *Journal of Non-Newtonian Fluid Mechanics*. 285(February): 104383. DOI: http://dx.doi.org/ 10.1016/j.jnnfm.2020.104383.

[39] Murali, C. and Nithiarasu, P. 2017. Red Blood Cell (RBC) Aggregation and Its Influence on Non-Newtonian Nature of Blood In Microvasculature. *Journal of Modeling in Mechanics and Materials*. 1(1). DOI: http://dx.doi.org/10.1515/jmmm-2016-0157.

[40] Qian, C., Huang, H., Chen, L., Li, X., Ge, Z., Chen, and T., Yang, Z. 2014. Dielectrophoresis for Bioparticle Manipulation. *International Journal of Molecular Sciences*. 15(10): 18281-18309. DOI: http://dx.doi.org/10.3390/ijms151018281.